Journal of Materials Science & Technology 32 (2016) 1204–1210

Contents lists available at ScienceDirect

Journal of Materials Science & Technology

journal homepage: www.jmst.org

Fracture Characteristics of Frit Bonding through *In-Situ* Nano-Indentation Testing

Won Je Jo *, Hee-Jun Ahn, Jong Hyoung Kim, Dongil Kwon

Department of Materials Science and Engineering, Seoul National University, Seoul 151-744, Republic of Korea

ARTICLE INFO

Article history:
Received 3 July 2015
Received in revised form
22 July 2015
Accepted 22 July 2015
Available online 15 September 2016

Key words:
Nanoindentation
Bonding
Fracture behavior

Because frit bonding material is brittle, sudden impacts such as dropping may damage the bonding significantly. Strain-rate-controlled *in-situ* nano-indentation testing, which can determine localized material properties, was carried out on the frit-bonded specimen, especially on the frit bonding matrix and the filler. The results were compared with the drop-impact fracture behavior to understand the fracture characteristics. Mechanical properties at static condition or low strain rate did not show proper relationship with the fracture tendency of the drop tested result of the frit bonding. From the relationship between fracture toughness and the ratio of modulus/hardness, fracture characteristics at the drop impact situation could be estimated by the values at the high strain rate nano-indentation. The ratio between modulus and hardness on frit matrix showed close relationship with drop impact fracture. Though crack propagation path deflected at filler interface, filler property gave less influence on fracture tendency of drop impact fracture due to its small volume fraction. The properties of frit matrix were crucial to the fracture characteristics of the frit bonding.

Copyright © 2016, The editorial office of Journal of Materials Science & Technology. Published by Elsevier Limited.

1. Introduction

Frit bonding is widely used to encapsulate micro-electromechanical systems on the wafer level; in particular, micro-electronic devices such as OLED, which contain organic illuminants, use frit bonding for encapsulation. Modification of conductive frit bonding to use conductive filler inside the bonding material is still being studied in many electronic industries[1–4]. Several industries have adopted printing techniques to produce frit bonding, which is versatile to build up various shapes and bonding thicknesses[1–7].

Frit bonding occurs at the atomic level, forming a hermetic seal, and it is thus considered to produce reliable bonding with high process yield strength and high bond strength[5]. It is therefore effective in encapsulating organic devices, which are generally susceptible to oxidation. Though glass-based bonding materials have high yield strength, they are brittle (like ordinary glass-based materials). Failure of frit bonding occurs in a brittle manner, in particular under impact stress such as dropping.

Many attempts have been made to improve fracture resistance of frit bonding using various analysis methods[8,9]. However, the generally accepted analysis of its fracture behavior is still qualitative due to lack of thickness (generally 10 μm) to get sufficient specimen size. Nanoscale indentation testing is the only way to get material data of the frit bonding. Mechanical properties acquired by nano-indentation could be applied to analyze the fracture characteristics of frit bonding, and those may suggest effective ways to improve toughness. Because most of the nano-indentation data are acquired at static strain rate rather than dynamic, it is hard to analyze fracture of brittle materials which usually occurs under dynamic condition.

In the present study the localized mechanical properties of commonly used frit bonding components, vanadium–tellurium- (V-T-), vanadium–phosphate- (V-P-) and Bi-based frit bonding, are evaluated through *in-situ* nano-indentation. Fracture tendency of the frit bonding was predicted on the basis of the mechanical properties measured by nano-indentation with various strain rates. Fracture tendency under drop impact test and predicted fracture toughness by substituting the measured data to the known equation have been compared with each other.

2. Theoretical Basis of Nano-Indentation

Generally, hardness implies a resistance to deformation. In addition, it is likely to indicate resistance to indentation[10]. It is generally known that the hardness of a material is closely related to its fracture characteristics. Especially for very brittle materials, previous experimental studies have verified that hardness is closely related to fracture toughness of the materials[11–15]. Thus, fracture properties of material can be deduced by evaluating mechanical properties with nano-indentation.

* Corresponding author.
E-mail address: maskofwdw@snu.ac.kr (W.J. Jo).

http://dx.doi.org/10.1016/j.jmst.2016.09.009
1005-0302/Copyright © 2016, The editorial office of Journal of Materials Science & Technology. Published by Elsevier Limited.

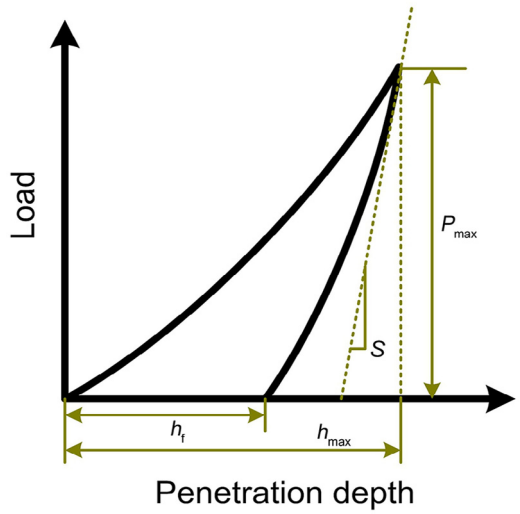

Fig. 1. Indentation load–displacement curve.

There are various methods to derive hardness depending on the shape of the indenter. A conventional method of measuring hardness is to define the maximum load per unit area. Oliver and Pharr[16] suggested defining indentation hardness independently from conventional hardness. Hardness can be measured by indentation load–depth curve from the residual indentation trace as shown in Fig. 1. The Oliver–Pharr indentation hardness is[16]:

$$H = \frac{P_{max}}{A} \tag{1}$$

where, H is hardness, P_{max} is maximum load, and A is contact area.

The indentation hardness method is more reliable in defining mechanical properties of materials than conventional method because indentation hardness is derived from the actual contact area, including both elastic deflection and plastic pile-up during indentation. For brittle materials such as ceramics and glass, only a little or no plastic deformation occurs, so that only elastic deflection is considered.

To calculate the actual contact area from the load–displacement curve, the real contact depth must be calculated. The real contact depth can be measured by subtracting the maximum contact depth and elastically recovered displacement, and then from the indenter area function, the contact area can be calculated:

$$h_c = h_{max} - h_d \tag{2}$$

$$h_d = \epsilon \frac{P_{max}}{S} \tag{3}$$

$$A = F(h_c) = C_0 h_c^2 + C_1 h_c + C_2 h_c^{\frac{1}{2}} + C_3 h_c^{\frac{1}{4}} + C_4 h_c^{\frac{1}{8}} + C_5 h_c^{\frac{1}{16}} \tag{4}$$

where, h_c is real contact displacement, h_d is elastic recovered displacement, h_{max} is maximum displacement, P_{max} is maximum load, C is constant for area function of cube corner tip.

Stiffness is measured from the unloading slope of load–displacement curve and the elastic modulus can be measured from the relation of stiffness and elastic modulus[17]:

$$\frac{1}{E_r} = \frac{1-\upsilon^2}{E} + \frac{1-\upsilon_i^2}{E_i} \tag{5}$$

$$E_r = \frac{1}{\beta}\frac{\sqrt{\pi}}{2}\frac{S}{\sqrt{A_c}} \tag{6}$$

where, E_r is effective Young's modulus, E is Young's modulus of specimen, υ is Poisson's ratio of specimen, E_i is Young's modulus of indenter, υ_i is Poisson's ratio of indenter, S is stiffness of specimen, A_C is real contact area, and β is indenter geometry factor

Doerner and Nix[18] suggested that various strain rate conditions can be created by controlling the indentation velocity. The indentation strain rate could be defined in terms of displacement using the load–displacement relations in indentation testing:

$$\dot{\varepsilon} = c\left(\frac{1}{h}\frac{dh}{dt}\right) \tag{7}$$

Mechanical properties tested in dynamic strain-rate situations, such as drop impact, can be measured by *in-situ* nano-indentation test with controlling loading rate. Cowper–Symonds devised a FEM simulated model of mechanical property difference versus various indentation strain rates according to the above definition of indentation strain rate[19].

Indentation techniques are widely applied for testing nano/micro-scale materials. In particular, the properties of thin substance such as frit bonding can be measured in nano scale with an *in-situ* nano-indentation device installed inside an SEM chamber.

3. Experimental

3.1. Specimen preparation

Specimens of three different glass-based materials were prepared. Three different glass-based materials, V-T (vanadium–tellurium), V-P (vanadium–phosphate) and Bi (bismuth), were used as the matrix material. Various commercially available additives were included in each matrix material to create complete frit bonding: EC (Ethyl cellulose), NC (Nitro cellulose), HPC (Hydroxypropyl cellulose), acryl-based binder and TPN (Terpineol), BCA (Butyl carbitol acetate), DBP (Dibutyl Phthalate) solvents were added as filler and binder.

The preparation process was the same for each specimen: after printing the paste (a mixture of bonding material and additive), its organic components were removed by a primary heat-treatment cycle of drying at 350 °C. During a second heat-treatment cycle at 420 °C, the paste was in the bulk state. To minimize the internal stress in the glass substrate during heating, hermetic sealing was completed by laser-assisted heating. Fig. 2 shows the fabricated frit bonding where filler of radius 2–3 μm is embedded in the base material with 10–20 μm in thickness.

3.2. Drop impact test

Drop impact tests were conducted for the prepared three kinds of the specimens. The specimens were dropped from 1.2 m height to the bottom of the proprietarily designed facility as shown in Fig. 3. Drop impact resistance was counted by number of total drops to failure of each face.

3.3. In-situ *nano-indentation testing*

In-situ nano-indentation test was conducted using PI85 (Hysitron) devices inside the chamber of a scanning electron microscope. Hardness and modulus, thought to be related to fracture properties, were measured for each constituent of the frit bonding materials (the filler and frit matrix) as shown in Fig. 4. Load-controlled indentation testing up to 5000 μN was performed using a cube-cornered indenter. Strain-rate-controlled indentation tests were carried out on base material in the strain rate range of 1 s^{-1} to 25 s^{-1}, which is the static to dynamic strain range. Crack morphology and microstructure of the frit bonding were observed by scanning electron microscopy (SEM, Quanta250).

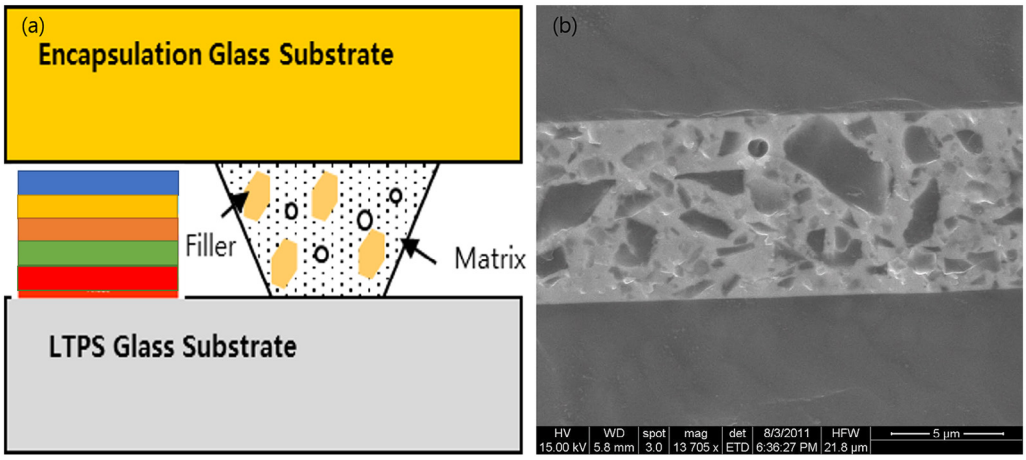

Fig. 2. Schematic structure of frit bonding (a), and SEM micrograph of frit bonding (b).

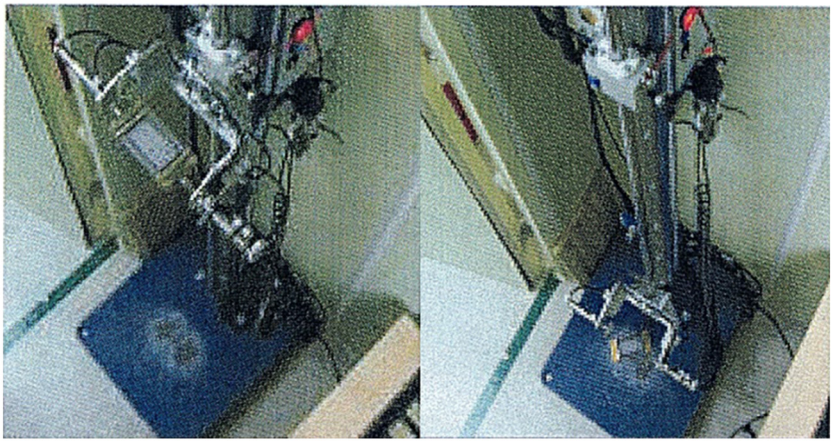

Fig. 3. Drop impact test apparatus.

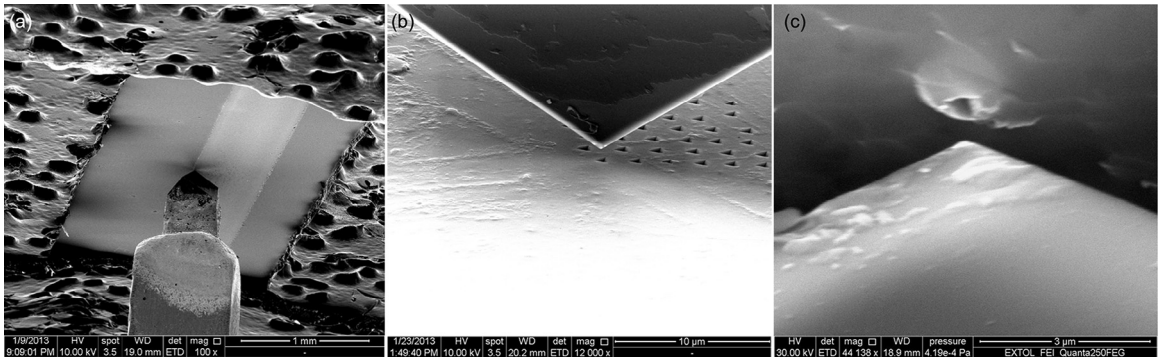

Fig. 4. *In-situ* nano indentation test (a) in the frit bonding matrix (b), and in the filler (c).

4. Result and Discussion

Due to rapid crack propagation in brittle materials crack initiation has a major role in total fracture behavior. Therefore, material properties such as fracture toughness, meaning the resistance to crack opening, would be crucial to cause total fracture of the material. Because of 10-µm thickness of frit bonding materials, it was impossible to conduct generally accepted fracture toughness test. Several studies have indicated that fracture toughness can be predicted by hardness value[11–15]. Nanoindentation tests were applied to measure mechanical properties to calculate fracture toughness through proved relationship suggested by Lawn et al.[12]. Hardness and elastic modulus of the frit bonding materials, including matrix and filler, were measured with indentation load–displacement curve as shown in Fig. 5, which were inputted to the equation to understand fracture characteristics of frit bonding.

The frit bonding is a kind of composite material. The hard particles in a composite material can affect the fracture behavior of the material, since crack propagation can be arrested by particles on the crack path. In composites, an increase in the hardness of the second particle may lead the material to tolerate from fracture. Similar to the role of second particles in polymer-based composite materials, crack propagation is dependent on the volume fraction and mechanical properties of the second particles. Thus, the material

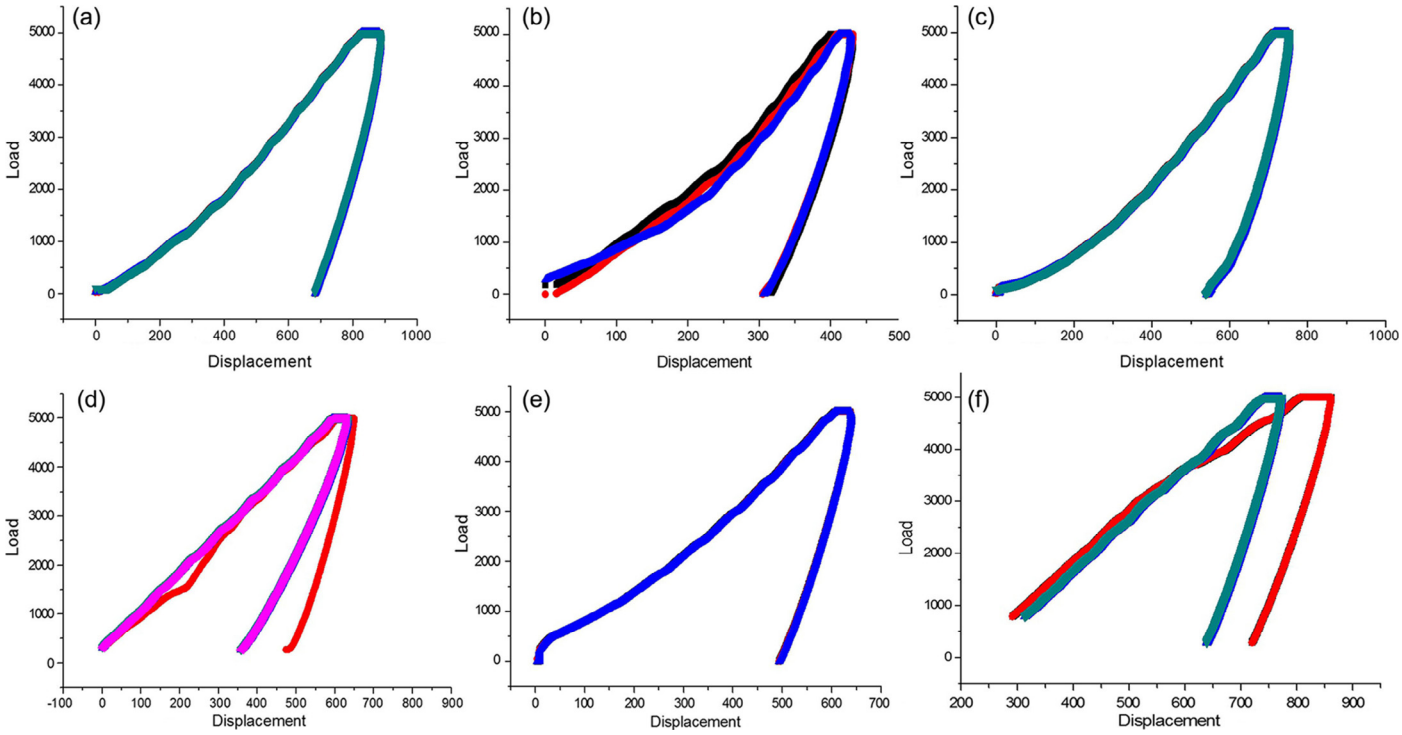

Fig. 5. Indentation load–displacement curves of frit material: (a) V-T-based frit bonding matrix; (b) V-T-based frit bonding filler; (c) V-P-based frit bonding matrix; (d) V-T-based frit bonding filler; (e) Bi-based frit bonding matrix; (f) Bi-based frit bonding filler.

properties of second particles may also have a role in crack propagation. The effect of the second particles on the resistance to fracture of the brittle material was also studied regardless of its volume fraction.

4.1. In-situ *nano-indentation on frit bonding matrix*

In-situ nano-indentation testing of the matrix showed that the hardness values for each frit bonding matrix were 2.56 ± 0.16 GPa, 2.67 ± 0.19 GPa, and 3.20 ± 0.13 GPa for the V-T-, V-P- and Bi-based frit bonding specimens, respectively. The Bi-based frit bonding specimen showed the highest hardness; the V-T- and V-P-based frit bonding specimens showed similar values. The above static hardness values have similar tendency to the drop impact fracture tendency. However, hardness value does not directly indicate fracture behavior. Therefore, the property related to fracture characteristics is necessary.

Due to existence of various defects at the interface of the bonded material, crack initiates preferentially at the interface and then followed by sudden propagation through the material. Interface of the bonding may behave as a stress concentration site like pre-crack in fracture toughness testing. The resistance to cracking is closely related to the fracture toughness of the material rather than hardness value. However, direct measurement of fracture toughness is impossible due to lack of material thickness as mentioned above. The fracture toughness value could be drawn from Eq. (8), which shows the relationship between fracture toughness and indentation hardness, suggested by Lawn et al.[12].

$$K_c = \alpha\left(\frac{E}{H}\right)^{\frac{1}{2}}\left(\frac{P_{max}}{c^{\frac{3}{2}}}\right) \tag{8}$$

where K_c is fracture toughness, H hardness, P load, c crack length.

The equation expresses K_c value under the existence of indentation crack. But in the present study the applied load during indentation was extremely low (5000 μN), thus crack did not appear clearly at the sharp corner of the indented trace as shown in Fig. 6. It was impossible to get the exact fracture toughness value. However, careful observation at the indented trace revealed crack-like morphology within the indented surface as indicated by arrows in Fig. 6. Thus, it is possible to adopt Eq. (8) which calculates fracture toughness even though the calculated values may not represent the exact K_c values. The extremely small loading left similar indented trace for each specimen though the hardness values were different from each other. It is possible to assume this small trace as a crack, and the length of the crack for each material is similar. Then, the trend of fracture toughness could be predicted by E/H ratio in Eq. (8).

The comparison of K_c values by substituting E/H ratio from Table 1 and Eq. (8) was relatively high for Bi, and similar for V-T- and V-P-specimens. This fracture toughness trend is totally different from that expected from the hardness values: the Bi-based bonding specimen

Table 1
In-situ nano indentation results of frit bonding specimen

	VT based bonding specimen					VP based bonding specimen					Bi based bonding specimen				
	E (GPa)	err	*H* (GPa)	err	*E*/*H*	*E* (GPa)	err	*H* (Gpa)	err	*E*/*H*	*E* (GPa)	err	*H* (GPa)	err	*E*/*H*
Filler	74.43	4.19	2.60	0.51	28.6	136.6	3.34	3.57	0.39	38.2	112.5	3.53	3.69	0.25	30.5
Matrix	50.35	2.65	2.56	0.16	19.6	49.4	3.98	2.67	0.19	18.5	68.79	3.39	3.20	0.13	21.5
Drop fracture resistance	High					Middle					Low				

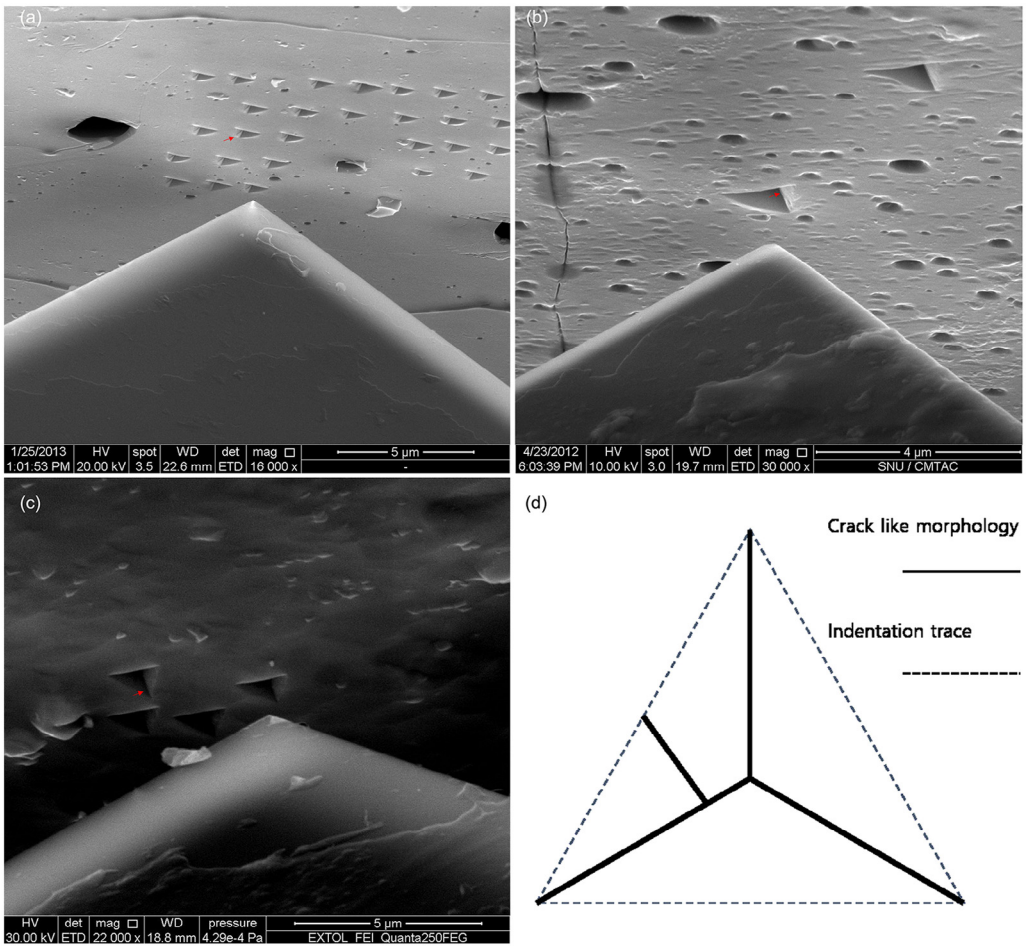

Fig. 6. Revealed crack like morphology within indented surface: V-T-based frit bonding; V-P-based frit bonding; (c) Bi-based frit bonding; (d) schematic of crack like morphology.

is expected to be more fragile than the V-T- and V-P-based frit bonding specimens. The data listed in Table 1 are acquired under static strain condition. Impact stress or fracture is a kind of dynamic strain condition. Thus, it was impossible to find the direct relationship between the static mechanical data of hardness and modulus with fracture tendency. Actually, drop impact test showed that it is relatively tough for V-T-, middle for V-P-, and brittle for Bi-based specimen as listed in Table 1. Because material behavior at drop impact test is related to the dynamic properties, the properties at high strain rate would be useful for the analysis of drop impact fracture.

4.2. *Strain rate controlled* in-situ *nanoindentation on frit bonding matrix*

Table 2 displays the hardness values and the modulus values at various strain rates (in the range of 1–25 s^{-1}). Generally, materials exhibit different mechanical properties and fracture behaviors depending on the strain rate. Drop-impact testing, which performs instantaneously and is similar to practical dropping situation of the electronic products, can be considered as a dynamic strain condition. In order to find the detailed relationship between drop-impact fracture tendency and the empirical data, the indentation test must be carried out under high strain rate conditions.

Doerner and Nix suggested that the strain rate during indentation testing can be controlled by the loading rate[18]. *In-situ* nanoindentation tests on the matrix were carried out in the strain-rate range from 1 s^{-1} to 25 s^{-1}.

The hardness values and the modulus values increased with increasing strain rate as shown in Table 2. The increased values mean that the materials have a certain sensitivity to strain rate as shown in Fig. 7. As mentioned above, fracture behavior could be evaluated by fracture toughness rather than hardness value. Fig. 8 displays evolution of E/H values with increasing strain rate. The value for each material decreased with increasing strain rate, and the decreasing

Table 2
In-situ nano indentation results with various strain rates

Strain rate (s)	VT based bonding specimen(matrix)					VP based bonding specimen(matrix)					Bi based bonding specimen(matrix)				
	E (GPa)	err	*H* (GPa)	err	*E/H*	*E* (GPa)	err	*H* (GPa)	err	*E/H*	*E* (GPa)	err	*H* (GPa)	err	*E/H*
1	50.35	2.65	2.56	0.16	19.66	49.46	3.98	2.67	0.19	18.52	68.78	3.39	3.20	0.12	21.46
10	51.35	3.27	2.62	0.26	19.59	51.12	1.84	2.71	0.04	18.86	65.42	3.12	3.50	0.22	18.66
15	53.22	1.23	2.82	0.02	18.87	53.72	1.63	2.86	0.02	18.78	67.88	1.33	3.94	0.11	17.22
25	69.34	5.766	3.63	0.3	19.10	72.21	1.76	4.12	0.26	17.52	69.22	1.44	4.43	0.13	15.62

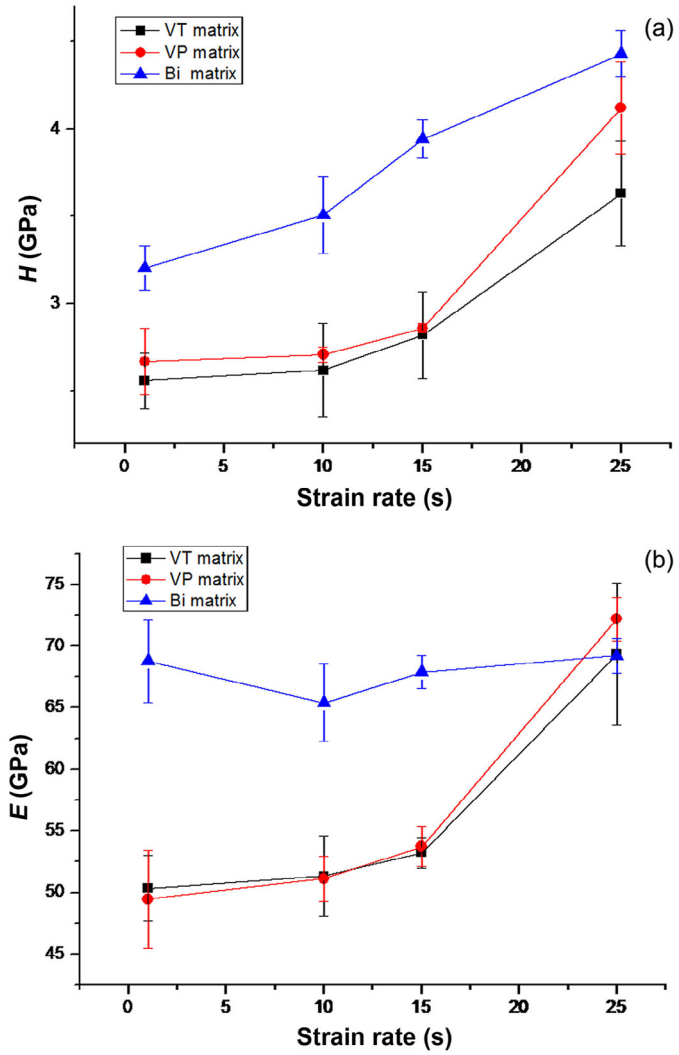

Fig. 7. Indentation hardness (a) and elastic modulus (b) with various strain rates.

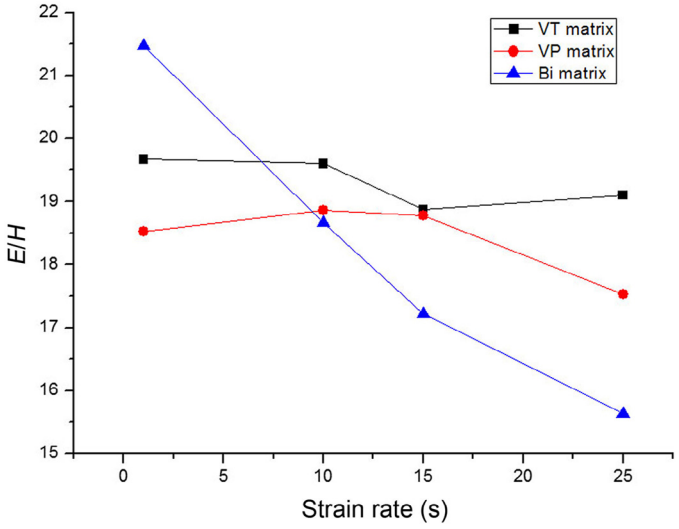

Fig. 8. *E*/*H* ratio with various strain rates.

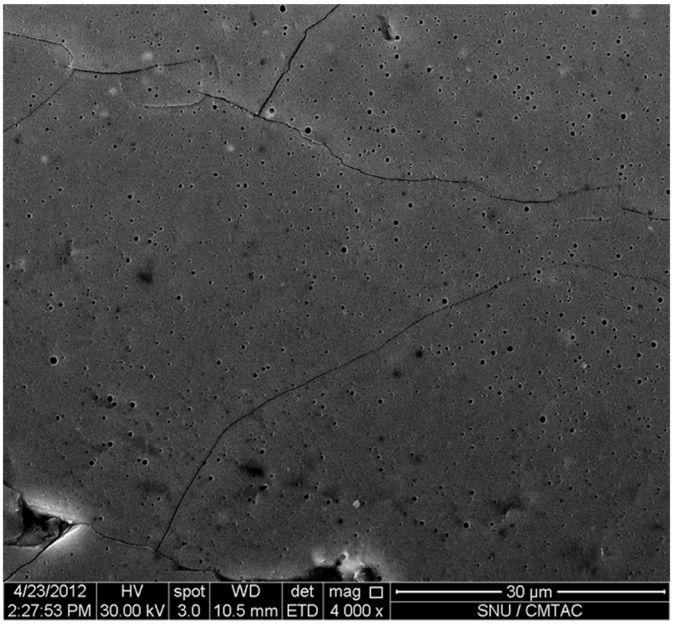

Fig. 9. Crack propagation of frit bonding matrix after drop impact test.

tendency was different from each other base material. At the highest strain rate of 25 s^{-1} *E*/*H* value of V-T matrix based frit showed most highest value and Bi matrix based frit showed the lowest value. K_c value could be calculated by substituting *E*/*H* in Eq. (8) for each material. This tendency is similar to the drop impact tendency as referred in Table 1. Thus, the results of *in-situ* nano-indentation testing at various strain rates clearly confirm that the mechanical properties of the matrix play a major role in the fracture behavior of frit bonding.

The approach that estimated dynamic fracture toughness with various strain rates cannot be found elsewhere except in the present study. The approach would be very effective to understand fracture behavior in conjunction with previous study of K_c conversion with indentation results.

4.3. In-situ *nano-indentation on filler material*

The effect of matrix properties on fracture behavior in terms of brittleness is discussed above. The resistance to crack propagation of the included particles is considered below. As mentioned above, fracture in frit bonding can be influenced not only by matrix material, where crack initiation and propagation occur, but also by the filler material, which controls thermal expansion rate of the whole body. Previous studies have suggested that the filler should work as a crack initiation point because of stress concentration at the sharp edge[1]. In addition, filler on the crack path may influence the propagation of the initiated crack depending on its properties.

The hardness and elastic modulus of the filler materials were measured with *in-situ* nano-indentation to verify those effects on bonding fracture tendency. The data are listed in Table 1. *E*/*H* values which could substitute K_c tendency, showed relatively high for Bi-based frit bonding specimen filler, middle for V-P-based frit bonding specimen filler, and low for V-T-based frit bonding specimen filler. It was expected that the filler properties may influence the tendency to fracture, just as particles in composite materials deflect or branch the crack propagation path. However, it was hard to find the distinct relationship between the *E*/*H* values and fracture tendency described in Table 1. Because crack initiated at the interface of the frit bonding followed by sudden propagation in the matrix, the crack may meet the filler particles on the propagation path. Fig. 9 shows the crack

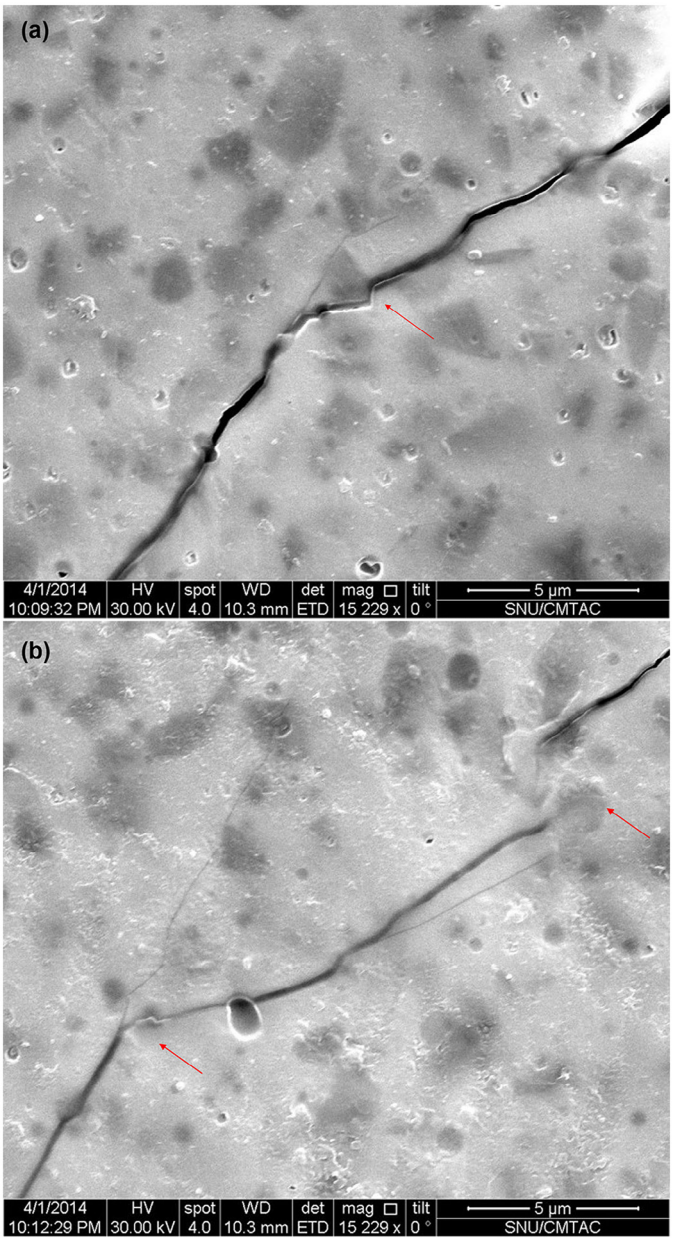

Fig. 10. Crack propagation in the matrix and along filler–matrix interface: (a) advancing crack deflected by filler particle; (b) crack branching occurred as the advancing crack met the filler particles.

propagation path in the drop-impact-tested frit bonding specimens. As expected, the initiated crack propagated primarily through the matrix and frequently met the filler. Sometimes the filler acted as a barrier to crack propagation: thus crack branching occurred as the advancing crack met the filler particles, as indicated in Fig. 10. Even though the filler particle deflected the crack propagation path, crack propagation is so rapid in brittle fracture that this deflection had little or no influence on the fracture tendency of the whole body, and moreover the volume fraction of the filler was not sufficient to prevent the fracture, In the present study, because the filler volume fraction was 30% for each of the three specimen types, only a little or no influence on fracture tendency or fracture behavior appeared. However, a high volume fraction of filler may have a significant effect on fracture behavior such as crack branching, as shown in Fig. 10.

5. Conclusions

(1) The properties of matrix material under static and dynamic loading conditions were crucial factors on the fracture characteristics of the frit bonding due to rapid crack propagation through the matrix regardless of base material.

(2) Hard matrix with high hardness value of static condition is expected to have low fracture toughness. However, the fracture characteristics were not always governed by the hardness value, but the fracture tendency was governed by the ratio between modulus and hardness value at high strain rate. Simulated drop impact condition of high strain rate nanoindentation test effectively estimated practical fracture tendency of the frit bonding.

(3) Though crack branching occurred along the filler–matrix interface, the effect of second particles on the fracture was not significant because of the relatively low volume fraction. The strain rate controlled nano-indentation is capable of evaluating the fracture tendency of brittle materials, which is useful to investigate the reliability of frit bonding.

References

[1] R. Knechtel, Microsyst. Technol. 12 (2005) 63–68.
[2] R. Knechtel, M. Wiemer, J. Frömel, Microsyst. Technol. 12 (2006) 468–472.
[3] F. Ribeiro, J. Marcaira, R. Cruz, J. Gabriel, L. Andre, A. Mendes, Sol. Energ. Mat. Sol. Cells 96 (2012) 43–49.
[4] K. Nötzold, J. Graf, R. Müller-Fiedler, Microelectron. Reliab. 48 (2008) 1562–1566.
[5] X. Chen, E. Dubois, F. Ravaux, F. Danneville, Microelectron. Eng. 100 (2012) 280–284.
[6] H.Y. Shin, W.S. Chung, K.H. Kim, Y.R. Cho, B.C. Shin, J. Vac. Sci. Technol. B 23 (2005) 2369–2372.
[7] D. Jang, D. Kim, B. Lee, S. Kim, M. Kang, D. Min, J. Moon, Adv. Funct. Mater. 18 (2008) 2862–2868.
[8] C. Dresbach, A. Krombholz, M. Ebert, J. Bagdhan, Microsyst. Technol. 12 (2006) 473–480.
[9] M. Petzold, C. Dresbach, M. Elbert, Thermal and thermomechanical phenomena in electronics systems, 2006.
[10] G.E. Dieter (Ed.), Mechanical Metallurgy SI Metric, McGraw-Hill, 1988, pp. 246–250.
[11] S. Palquist, Jernkontorest Ann. 141 (1957) 300–307.
[12] B.R. Lawn, A.G. Evans, D.B. Marshall, J. Am. Ceram. Soc. 63 (1980) 574–581.
[13] K. Niihara, R. Morena, D.P.H. Hasselman, J. Mater. Sci. Lett. 1 (1982) 13–16.
[14] M. Sebastiani, K.E. Johanns, E.G. Herbert, G.M. Pharr, Current opinion in solid state and materials science, 2015.
[15] Y. Feng, T. Zhang, Acta Mech. Solida Sin. 38 (2015) 221–234.
[16] W.C. Oliver, G.M. Pharr, J. Mater. Res. 7 (1992) 1564–1583.
[17] I.N. Sneddon, Int. J. Eng. Sci. 1 (1965) 47–57.
[18] M.F. Doerner, W.D. Nix, J. Mater. Res. 1 (1986) 601–609.
[19] G.R. Cowper, P.S. Symonds, Applied mathematics report RI, 1958, pp. 1–46.